Effect of Silicon and Phosphorus on the Degradation of Polyurethanes

MING-FUNG LIN,[1] WEN-CHIN TSEN,[2] YAO-CHI SHU,[2] FU-SHENG CHUANG[1]

[1] Department of Textile Engineering, Feng Chia University, Taichung, Taiwan 407, Republic of China

[2] Department of Textile Engineering, Van Nung Institute of Technology and Commerce, Tao-Yuan, Taiwan 320, Republic of China

Received 29 November 1999; accepted 5 April 2000

ABSTRACT: A series of polyurethanes containing silicon and phosphorus was prepared from 4,4′-diphenylmethane diisocyanate (MDI), poly(tetramethylene ether glycol) (PTMG), diphenylsilanediol (DSiD), and methylphosphonic acid (MPA). ^{1}H-NMR spectra determined the qualitative and quantitative characteristics of these polymers. The thermal stability and activation energy for thermal degradation of these polymers were measured by thermogravimtry and compared with pure polyurethane (PU). The DSiD incorporated into the main chain of the polymer improved the thermal stability of PU, while the phosphorus-containing polyurethane (P–PU) displayed a lower thermal stability than that of pure PU. The activation energies at various degradation stages for the pure PU, silicon-containing polyurethane (Si–PU), and P–PU polymers were calculated by the Ozawa method. The activation energies of the Si–PU polymers were higher than were those of pure PU and increased according to the increase in the DSiD content. However, the P–PU polymers' activation energies were smaller than were those of pure PU, and they decreased with increasing phosphorus content in the range of $0.1 \leq$ conversion ≤ 0.5, whereas the reverse was true between 0.6 and 0.9. © 2000 John Wiley & Sons, Inc. J Appl Polym Sci 79: 881–899, 2001

Key words: silicon; phosphorus; polyurethane; degradation

INTRODUCTION

The practical application of polymers requires materials that can resist a variety of external stresses such as heat, fire, acid, base, moisture, friction, and environmental contaminants. Polyurethanes (PUs) are an excellent material for withstanding external stresses such as providing water, chemical, and solvent resistance.[1–3] However, pure PUs have a lower thermal stability at high temperatures and thermal degradation occurs at processing temperatures above 200°C, depending on the hard- and soft-segment concentration as well as on the type of isocyanate and alcohol.[4] The onset degradation temperature was around 200°C for pure PUs formed from aryl isocyanate with an alkyl alcohol reaction.[5,6] urthermore, these pure PUs are seldom employed for resistance to harsh environmental exposure; however, they are flammable. Therefore, the thermal stability and flammability of PUs were extensively studied herein.[7–10] Indeed, chemical or physical processes can modify the thermal stability and flammability of materials.

The incorporation of aromatic imide or PmIA can promote the thermal stability of PU.[5,11] Sili-

Correspondence to: M.-F. Lin.

Contract grant sponsor: National Science Council of the Republic of China; contract grant number: 87-2216-E-238-003.

Journal of Applied Polymer Science, Vol. 79, 881–899 (2001)

con was utilized for cable application because of its resistance against high temperature, ozone, corona, and weathering. Moreover, silicon is nonhalogen and noncorrosive and gives minimal smoke on fire exposure. Siliconated PU shows great improvement in acid/base and solvent resistance[12] and excellent thermal stability and mechanical properties.[13,14] The flammability of polymers on fire exposure may be achieved by employing additive-type stabilizers and flame retardants or by improving its structure.[15,16] The flame retardancy of siliconated polymer can be enhanced[17–19] and the incorporation of a silicone moiety into the structure of polyimide increases its thermal stability.[20,21] The phosphorous compounds were utilized to promote the stabilization of a polymer, such as PU, poly(methyl methacrylate), epoxy, and polyester, against combustion.[22–25]

The activation energies of pure PU and phosphorus-containing polyurethane (P–PU) polymers in the thermal degradation processes have been thoroughly investigated.[22,26] However, the activation energies of silicon-containing polyurethane (Si–PU) polymers have not yet been evaluated and compared with those of P–PUs and the pure PUs. In this study, the Si–PU polymers, P–PU polymers, and silicon and phosphorus-containing PU (Si–P–PU) were prepared by a two-step process herein. Thermogravimetric analysis (TGA) was performed to examine how silicon and phosphorus contents affect the thermal stability and activation energy (Ea) of the degradation of the polymers.

EXPERIMENTAL

Materials

The 4,4′-diphenylmethane diisocyanate (MDI) (Aldrich, Poole, UK) was employed without further purification. The poly(tetramethylene ether glycol)s PTMG1000 and -2000 have 56 and 112 ($\overline{M_w}$ = 2000 and 1000), hydroxy (DuPont, Wilmington, DE), respectively, and were heated before use to 90°C for 4 h to restore the moisture content to 15 ppm. The chain extender, 1,4-butanediol (BD), and the solvent, *N,N*-dimethylformamide (DMF), were purchased from Merck (Berlin, Germany). Diphenylsilanediol (DSiD) and methylphosponic acid (MPA) were purchased from TCI (Tokyo, Japan) and Lancaster (Lancashire, UK), respectively.

Preparation of the Polymers

The concentrated DMF solution of Si–PU and P–PU polymers (30.0 wt %) was prepared by a two-step process adopting MDI, PTMG (1000 or 2000), a chain extender (DSiD, MPA, BD), and DMF. A 500-mL reaction flask equipped with a stirrer, a dropping funnel, and two-way cocks were employed for the polymerization.

The MDI and the macrodiol (PTMG1000 or PTMG2000) ([NCO]/[OH] = 2 molar ratio) were prepolymerized in DMF at 70°C under nitrogen to produce a 35 wt % PU prepolymer with an isocyanate end group (NCO-terminated prepolymer solution). The reaction was steadily stirred utilizing PTMG1000 and PTMG2000 for 60 and 80 min, respectively. After titrating the residual NCO group in the solution prepolymer using di-*n*-butylamine, a DMF solution of the chain extender DSiD or MPA equivalent to the NCO group was quickly added and stirred for 1.5 h to obtain the Si–PU polymer or P–PU polymers. The 1,4-BD replaced a part of DSiD or MPA in the chain-extending reaction because of various silicon contents or phosphorus contents in the polymers. The polymerization of Si–P–PU polymers resembled the reaction of Si–PU and P–PU, but the DSiD and MPA were also added to the chain-extending reaction. Those polymers were carefully placed into a Teflon mold and cast into films from the polymer solution for 24 h at 100°C. Scheme 1 presents those polymers' polymerization as a two-step process. The intrinsic viscosities of the samples were measured in DMF with an Ostwald U-tube viscometer at 30°C. Those samples of weight-average molecular weight ranged between 5×10^4 and 6.5×10^4 according to eq. (1). The equation was based on light-scattering data on a PU of similar composition.[27] Various polymer samples with varying contents of silicon and phosphorus were produced for investigating the effect of silicon and phosphorus on the degradation processes, and Table I lists the molar ratios and the various chemical compositions.

Measurements

NMR

^{1}H-NMR spectra were recorded on a Bruker AM-400 NMR spectrometer (^{1}H frequency of 400 MHz) and were measured for a 15% wt/vol solution of these polymers in d_6-DMSO (Aldrich) at 100°C. Tetramethylsilane was applied as the internal standard (0 ppm).

$$[\eta] = 6.8 \times 10^{-5} \overline{Mw}^{0.86} \quad \ldots\ldots\ldots\ldots (1)$$

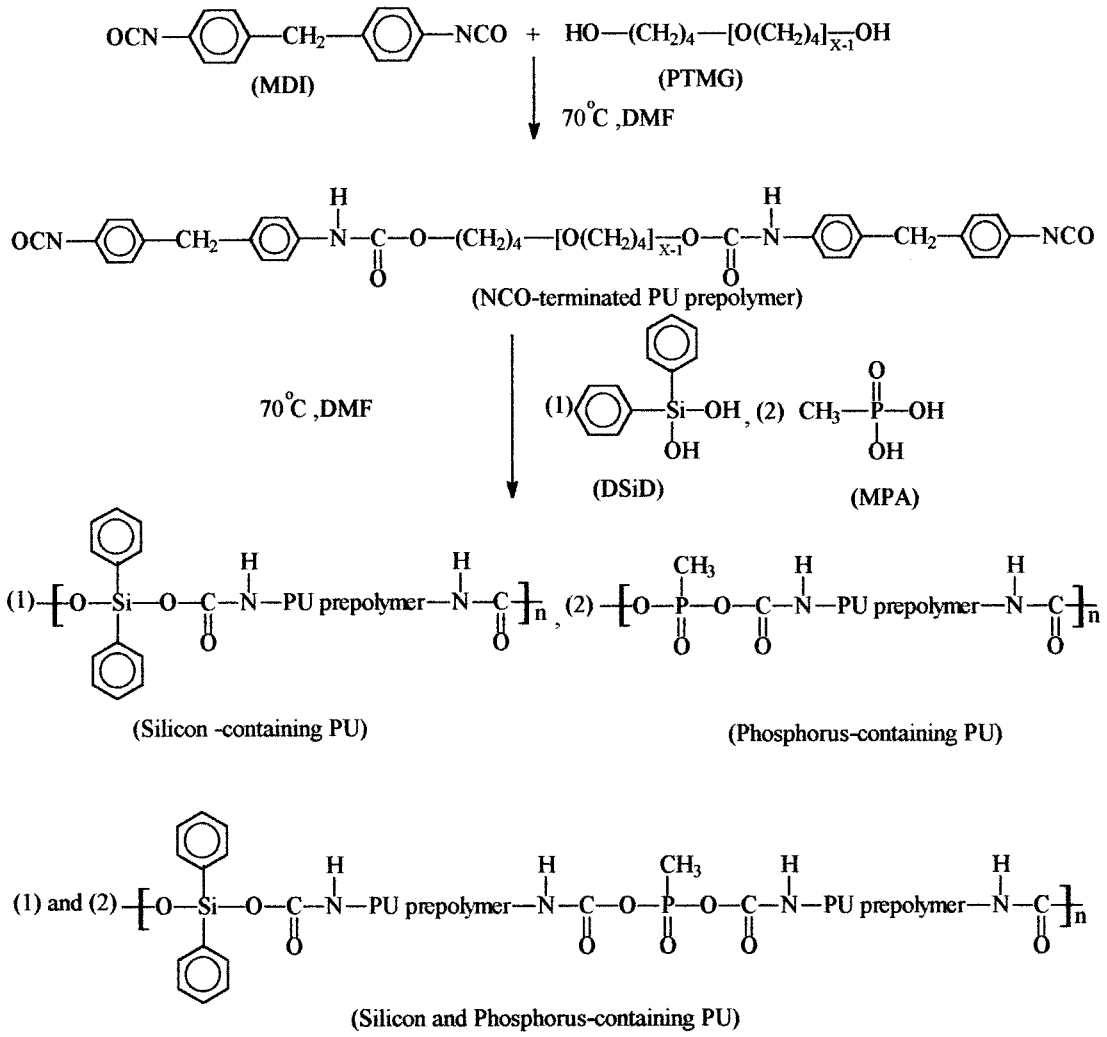

Scheme 1

Thermogravimetric Analysis (TGA)

A Seiko SSC 5000 TG/DTA instrument analyzed the characteristics and kinetics of the degradation of the samples. All the samples were roughly 10 mg as measured starting from room temperature to 600°C. A heating rate of 5, 10, 20, and 40°C/min were employed, while the nitrogen flow rate was calibrated at 100 mL/min.

RESULTS AND DISCUSSION

NMR Analysis

The qualitative and quantitative characteristics of the polymers were determined by ^{1}H-NMR spectra. The chemical-shift data for the structures and groups of those polymers interpreted from the spectra are presented in Table II. Although many methylene groups are chemically identical, their protons are not magnetically equivalent. Complex multiple patterns can also arise due to strong coupling. The X—$CH_2CH_2CH_2CH_2$—X structure occurs in PTMG and 1,4-BD, so the higher-field multiplet is attributable to the internal methylene group, and its chemical shift is less influenced by X than is the adjacent methylene.[28] Thus, the internal methylene group displayed chemical shifts of 1.50–1.59 or 1.62–1.65 and 1.67–1.71 ppm for PTMG and 1,4-BD, respectively, as illustrated in Figure 1(a,d). However, the adjacent methylene group displayed

Table I All of the Polymers' Molar Ratios of Synthesis in Stoichiometric Amount and the Content of DSiD and MPA

Code	Component	Molar Ratio	DSiD Content (wt %)	MPA Content (wt %)	[Urethane/MDI][a]
PU1	T1[b]/MDI/BD	1/2/1	—	—	0.87
PD11	T1/MDI/DSiD	1/2/1	12.6	—	0.92
PD12	T1/MDI/DSiD/BD	1/2/0.75/0.25	9.6	—	0.93
PD13	T1/MDI/DSiD/BD	1/2/0.5/0.5	6.5	—	0.94
PD14	T1/MDI/DSiD/BD	1/2/0.25/0.75	3.3	—	0.92
PM11	T1/MDI/MP	1/2/1	—	6	0.90
PM12	T1/MDI/MP/BD	1/2/0.75/0.25	—	4.5	0.94
PM13	T1/MDI/MP/BD	1/2/0.5/0.5	—	3	0.91
PM14	T1/MDI/MP/BD	1/2/0.25/0.75	—	1.5	0.95
PDM11	T1/MDI/DSiD/MPA	1/2/0.75/0.25	6.42	0.90	0.90
PDM12	T1/MDI/DSiD/MPA	1/2/0.5/0.5	6.5	2.8	0.93
PDM13	T1/MDI/DSiD/MPA	1/2/0.25/0.75	2.10	2.82	0.93
PU2	T2[c]/MDI/BD	1/2/1	—	—	0.95
PD21	T2/MDI/DSiD	1/2/1	8	—	0.94
PD22	T2/MDI/DSiD/BD	1/2/0.75/0.25	6	—	0.94
PD23	T2/MDI/DSiD/BD	1/2/0.5/0.5	4	—	0.95
PD24	T2/MDI/DSiD/BD	1/2/0.25/0.75	2	—	0.93
PM21	T2/MDI/MPA	1/2/1	—	3.7	0.91
PM22	T2/MDI/MPA/BD	1/2/0.75/0.25	—	2.8	0.94
PM23	T2/MDI/MPA/BD	1/2/0.5/0.5	—	1.9	0.92
PM24	T2/MDI/MPA/BD	1/2/0.25/0.75	—	0.9	0.94
PDM21	T2/MDI/DSiD/MPA	1/2/0.75/0.25	3.58	0.51	0.92
PDM22	T2/MDI/DSiD/MPA	1/2/0.5/0.5	4.1	1.8	0.91
PDM23	T2/MDI/DSiD/MPA	1/2/0.25/0.75	1.18	1.58	0.94

[a] The protons' proportion value of [urethane/MDI] measured by NMR.
[b] T1 = PTMG1000.
[c] T2 = PTMG2000.

chemical shifts of 4.05–4.08 and 4.10 ppm when it was adjacent to a urethane group. The diisocyanate portion of PU was identified by the NMR spectra and there was a clear CH_2 resonance at 3.78–3.8 ppm and the aromatic protons were active at 7.30–7.34 and 7.04–7.06 ppm for MDI as illustrated in Figure 1(a).

The qualitative characteristics of these Si–PU and P–PU polymers were similar to those of PU in the NMR spectra. However, the aromatic protons of DSiD of Si–PU and Si–P–PU centered at 7.0–7.59 ppm were displayed in many complex multiplet patterns [Fig. 1(b,d)]. MPA methyl presents a chemical shift of 1.20 ppm (three peaks) for P–PU and Si–P–PU [Fig. 1(c,d)]. The two peaks at 9.1–9.2 ppm were attributed to the urethane linkage proton. The peak at 9.16 ppm is that of the urethane between PTMG and MDI or the urethane proton between MDI and the chain extender (DSiD or MPA). The polymers can be quantitatively analyzed by applying the integral intensities of the resolved groups of resonances. The spectra of the urethane proton and the proton of CH_2 of MDI are especially useful for these polymers in this study during the protons of the urethane linkage formed by MDI, PTMG, and the chain extenders of diol. The proportion between the protons of CH_2 of MDI and the protons of the urethane linkage should, theoretically, equal 1 after reaction since the synthetic mol ratio of [NCO]/[OH] equals 1 (including MDI, PTMG, and the chain extender). Figure 1(a–d) illustrates that the significant peaks are 3.8 ppm (CH_2 protons of MDI) and 9.1–9.2 ppm (protons of urethane). Their protons' proportion value (urethane/MDI) is approximately the exact ratio of 1, which supports the proposed chemical structure and stoichiometry of these polymers as displayed in Table I.

Table II Structure and Group of Chemical-Shift Data for All Samples

Structure	Group	Chemical Shift (ppm)	Code[a]
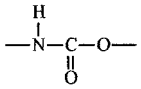	Urethane protons between PTMG and MDI	9.16	1
	Urethane protons between MDI and BD or DSiD or MPA	9.13–9.14	2
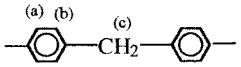	Aromatic protons of MDI	(a) 7.30–7.40	3
		(b) 7.04–7.10	4
	Methylene protons of MDI	(c) 3.78–3.79	5
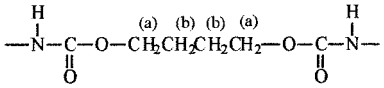	Methylene of BD adjacent to an urethane group	(a) 4.10	6
	Internal methylene of BD adjacent to an urethane group	(b) 1.67–1.71	7
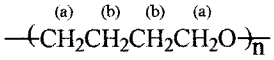	Methylene of PTMG adjacent to an ether group	(a) 3.33–3.39	8
	Internal methylene of PTMG adjacent to an ether group	(b) 1.50–1.60	9
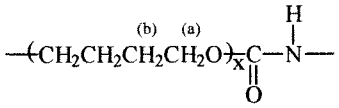	Methylene of PTMG adjacent to an urethane group	(a) 4.05–4.08	10
	Internal methylene of PTMG adjacent to an urethane group	(b) 1.61–0.66	11
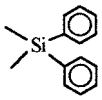	Aromatic protons of DSiD	7.04–7.6	12
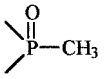	Methyl of MPA	1.14–1.25	13

[a] These numbers are the code of polymers group's chemical shift in the figure of the NMR spectrum.

Thermal Analysis

PU Polymers

A typical weight loss (TGA), differential weight loss (DTG), and differential thermal analysis (DTA) curve for the PU1 polymer at a heating rate of 10°C/min under nitrogen are displayed in Figure 2. The PU1 TG curve reveals that the onset temperatures of the first and second steps (T1on and T2on) were 220 and 369°C as presented in Figure 2(a). The onset degradation of PU is a depolymerization resulting from the dissociation of the urethane segments.[29,30] The TG curve reveals two distinct regions of weight loss [Fig. 2(a)], which were reflected in two peaks in the DTG curve [Fig. 2(b)]. Figure 2(c) demonstrates that the PU1 thermal decomposition processes are accompanied by heat absorption at around 305 and 399°C. Figure 2 clearly displays that at least two stages of degradation occur at the PU. Furthermore, the TGA of PU2 is similar to that of PU1.

Si–PU Polymers

The TG–DTG–DTA curves for the PD11 copolymer, with a PTMG chain length of 1000 and a DSiD content 12.6 wt %, exhibit three distinct regions of weight loss [Fig. 3(a)] that are reflected in three peaks in the DTG curve [Fig. 3(b)]. The degradation of the first and second steps is accompanied by heat absorption as illustrated in Figure 3(c). Moreover, the DTA curve [Fig. 3(c)] demonstrates that the third peak of heat absorption was around 440–500°C, which corresponds to the third weight-loss process. The degradation process resulted from the decomposition of silicone segments which produced volatile cyclic oligomers.[31–33] Figure 4 displays the TG–DTG–DTA curves of sample PD21, with a PTMG chain

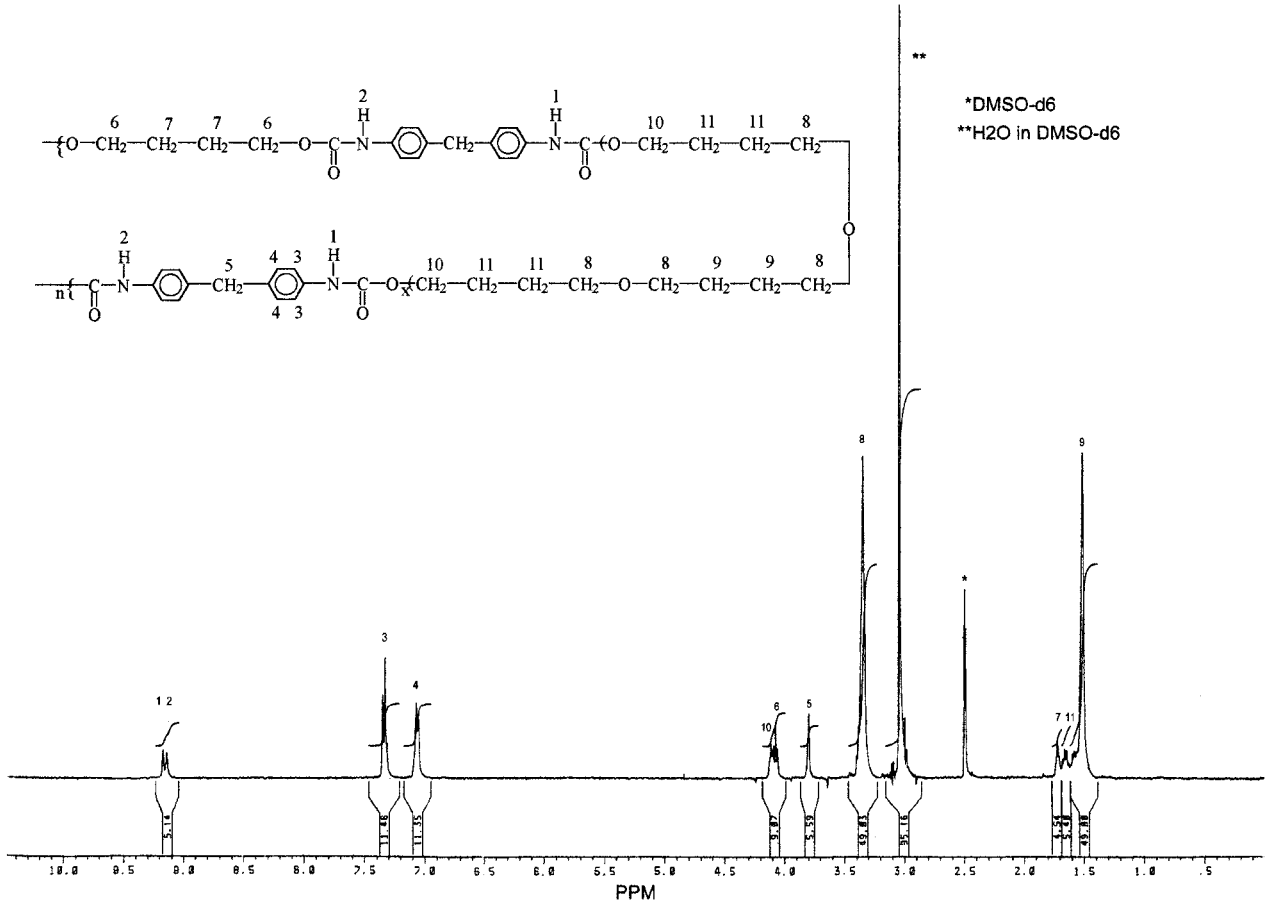

Figure 1 (a) Structure formula of PU1 and ^{1}H-NMR spectrum of PU1 measured at 100°C (TMS = 0 ppm). (b) Structure formula of PD11 and ^{1}H-NMR spectrum of PD11 measured at 100°C (TMS = 0 ppm). (c) Structure formula of PM11 and ^{1}H-NMR spectrum of PM11 measured at 100°C (TMS = 0 ppm). (d) Structure formula of PDM12 and ^{1}H-NMR spectrum of PDM12 measured at 100°C (TMS = 0 ppm).

length of 2000 and a DSiD content 8 wt %, which displays two distinct weight-loss regions and two DTG peaks. However, the DTA curve [Fig. 4(c)] has three areas of heat absorption at about 325, 420, and 470°C; the heat-absorption temperatures are lower than are the temperatures of the PD11 sample [Fig. 3(c)]. The third peak of heat absorption around 470°C also belongs to the decomposition of silicon segments. Although Figure 4(a,b) do not obviously display the third degradation step, the PD21 sample probably performs the process because of the effect of the DSiD content and the molecular weight of the soft segment. Furthermore, the degradation of the samples of various silicon components at the same length of the soft segment closely resemble PD11 and PD21. Thus, the Si–PU polymers underwent at least three degradation stages.

P–PU Polymers

Figures 5 and 6 display the TG–DTG–DTA curves of PM11 and PM21 with an MPA content of 6 and 3.7 wt %, respectively. The TG curve of PM11 [Fig. 5(a)] reveals three distinct weight-loss regions that are reflective of the three peaks in the DTG curve [Fig. 5(b)]. However, the TG curve of PM21 [Fig. 6(a)] displays only two distinct weight-loss regions that are reflective of two obvious peaks and a range of small multipeaks around 330–410°C as displayed in Figure 6(b). The PM11 and PM21 degradation processes are also accompanied by heat absorption as depicted in Figures 5(c) and 6(c). However, PM21, with a range of multiabsorption peaks about 334–438°C, differs from PM11 with only one broad absorption peak around 356°C. The effect of

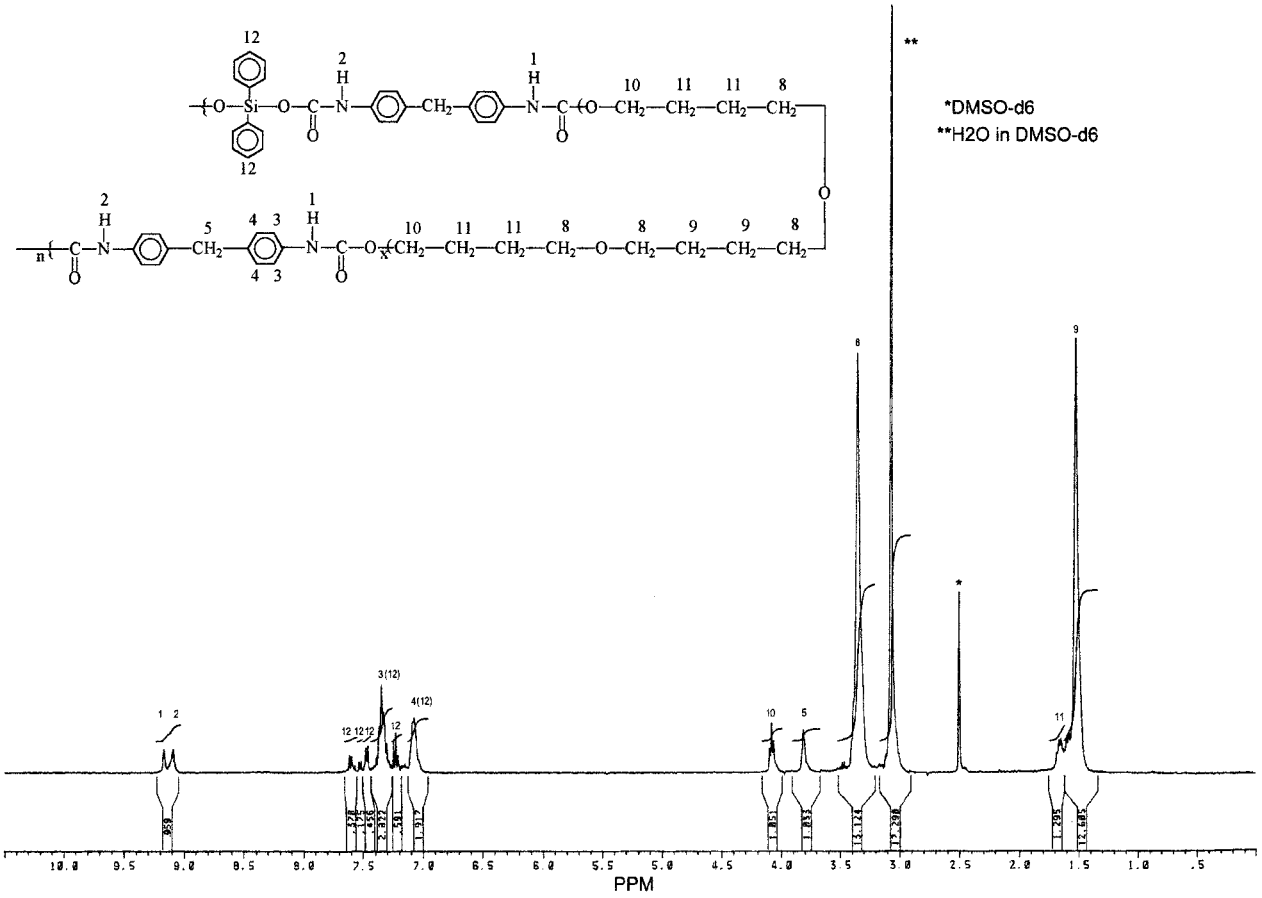

Figure 1 (*Continued from the previous page*)

small multipeaks and multiabsorption peaks may be attributed to bubble formation and bursting, which is related to the MPA content. Figure 7 demonstrates that those DTA curves are gradually close to forming one peak with the decreasing MPA content. Comparing the thermal stability among those samples (PD11, Pm11, and PU1) demonstrates that PM11 has the lowest thermal stability as depicted in Figure 8. The characteristic temperatures are often difficult to determine from the curves since the phosphorus content can affect the TGA.

Qualitative Characterization

The degradation process is qualitatively characterized by the onset and maximum temperature of the first step (T1on and T1m) and also for the second step, (T2on and T2m) and the third step (T3on and T3m). Table III(a–d) lists the characteristic temperatures of degradation for those samples at a 10°C/min heating rate under a nitrogen atmosphere. The T1on of the Si–PU polymers between 266 and 230°C exceeded those of the pure PU (PU1 and PU2) polymers at approximately 220–222°C and increased according to increase of the DSiD content as displayed in Table III(b). Similarly, the T2on of the Si–PU polymers also surpassed those of the pure PU polymers, but the DSiD content did not, obviously, affect the T2on of the Si–PU polymers at the same soft segment. Furthermore, the chain length of the soft segment also affected the temperature of onset degradation of various stages, except for the effect of the DSiD content. The T1on of the Si–PU polymers adopting PTMG 1000 (Si–PU1) was higher than that of the Si–PU polymers applying PTMG 2000 (Si–PU2). However, the chain length of the soft segment had an insignificant affect on the Si–PU polymers of T2on, whose temperatures were about 386–289°C (utilizing PTMG1000) and 373–378°C (utilizing PTMG2000).

The maximum temperature for each degradation stage is a character of the maximum degradation rate at various degradation stages. Table III(b)

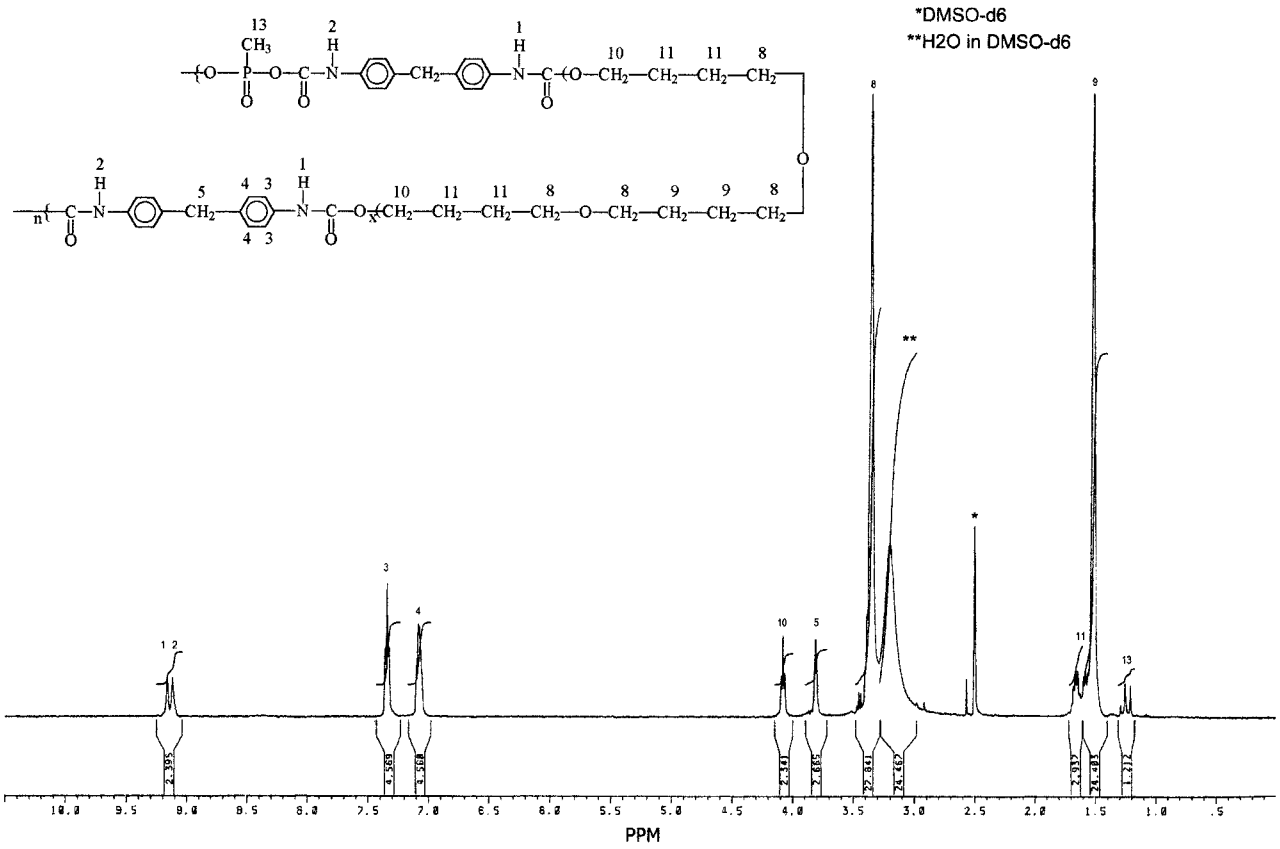

Figure 1 (*Continued from the previous page*)

demonstrates that the T1m and T2m of the Si–PU polymers exceeded those of the pure PU polymers. Furthermore, the Si–PU polymers with a high DSiD content had higher maximum temperatures. The T3on and T3m displayed only the Si–PU1 polymers for the Si–PU polymers, which may be related to the DSiD content and PTMG's molecular weight. The char residue at 500°C (*Yc*) of the Si–PU polymers is higher than that of PU due to the stable silicide product. Therefore, incorporating DSiD can enhance the thermal stability of PU.

Table III(c) displays the qualitative characterization of the P–PU polymers for each degradation step. The T1on's of various P–PU polymers around 169–204°C were lower than those of the Si–PU polymers and the pure PUs. Moreover, the T1on declined as the MPA content increased [Table III(c)], which reveals the poor thermal stability of the P–PU polymers. This result can be attributed to the phosphorus-containing segment, which readily produces thermal degradation.[23] The T2on and T3 of various P–PU polymers with a PTMG2000 chain length (P–PU2) were difficult to evaluate since the second and third steps were not obvious on the TG and DTG curves. However, the T2on and T3on of the P–PU polymers adopting PTMG 1000 (P–PU1) were clearly marked on the TG and DTG curves. The T2on of P–PU1 increased as the MPA content decreased, whereas the T3on slightly increased as the MPA content increased as presented in Table III(c). The T1m at 296–357°C and the T2m between 359 and 388°C of the P–PU1 polymers decreased as the MPA content increased, while the reverse occurred for T3m. The third step differs from the degradation of the first and second steps, which may be due to the formation of a thin glassy layer or liquid protective coating of polyphosphate on the condensed phase.[34] Similarly, the T1m and T2m could not be evaluated for P–PU2 because the DTG curve presented multiabsorption peaks. Furthermore, the maximum temperatures (Tm1, Tm2, and Tm3) of the P–PU1 polymers were lower than were those of Si–PU1, which indicated that the P–PU1 polymers will degrade faster at a lower temperature. The char residue of the P–PU polymers was obviously higher than that of the pure PU, and it increased with an increase in the MPA content

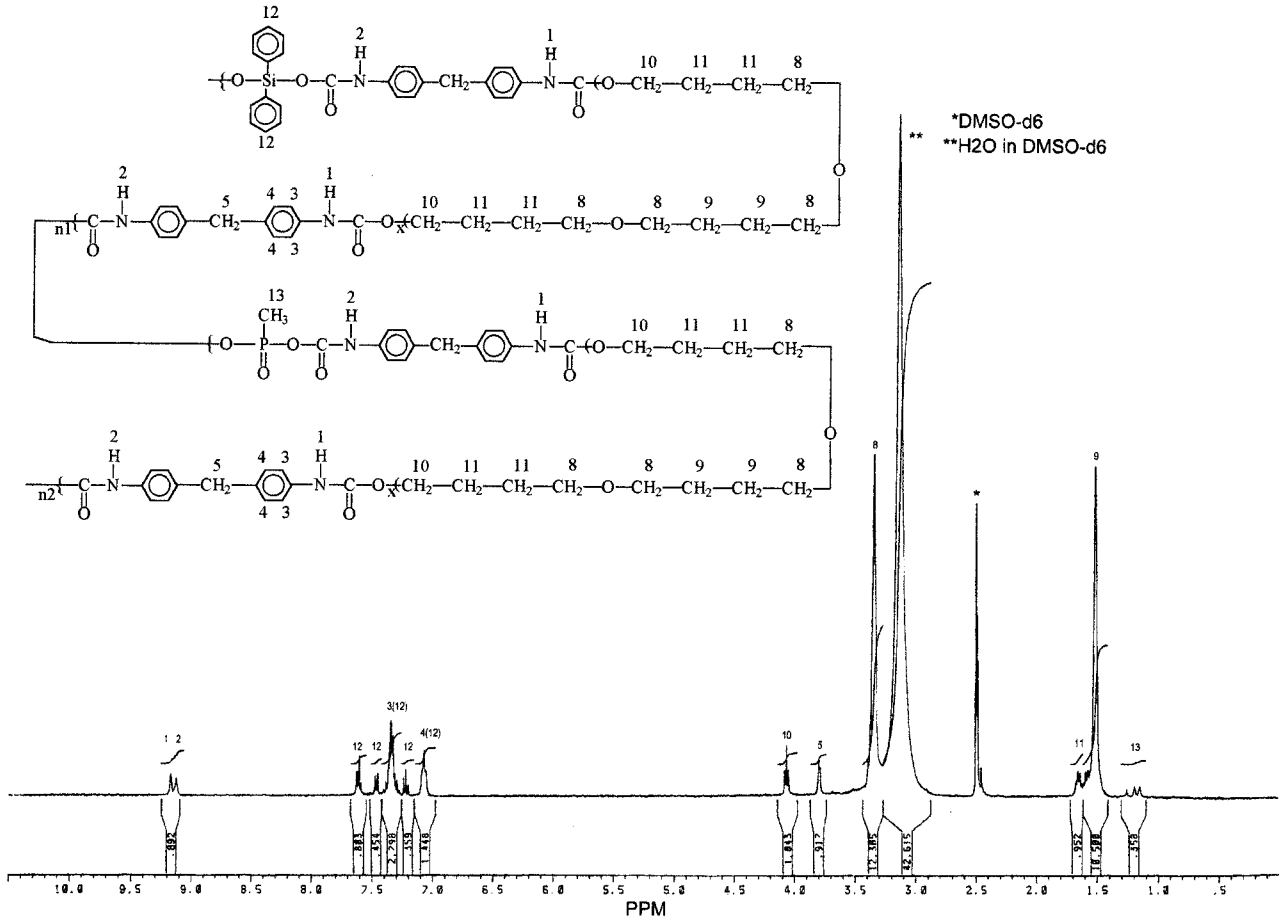

Figure 1 (*Continued from the previous page*)

because phosphorus forms anhydrides of phosphoric and acids that acted as dehydration agents that promoted char formation.[35,36]

Si–P–PU Polymers

The P–PU polymers have a low T1on from 170 to 200°C, which is disadvantageous to textile processes such as dying and finishing, even if the P–PU polymers are flame retardant. Incorporating silicon may increase the thermal ability of PU, so both phosphorous and silicon are simultaneously introduced into the main chain of the PU polymer. Therefore, the modified PU may be suitably thermally stable and flame retardant and the effect of the synergism of silicon and phosphorus on the degradation can be investigated.

The TG curve of the PDM12 polymers was between PD11 and PM11 and close to PU1 (Fig. 8), which verifies that the Si–P–PU polymers are more thermally stable than are the P–PU polymers and are closer to pure PU. Incorporating silicone can reduce the effect of the fast degradation of the phosphorus collocating to the pure PU. The TG curve of Si–P–PU (PDM12) reveals three distinct weight-loss regions [Fig. 9(a)] that do not reflect the three peaks on the DTG curve [Fig. 9(b)]. The DTG curve exhibited a split multipeak of two regions and a plateau region around 402–439°C, which were accompanied by multiabsorption peaks of two regions as illustrated in Figure 9(c). The split multipeak may be affected by phosphorus because the temperature range of the split multipeak was also displayed on the DTG and DTA curves of the P–PU2 polymers. Moreover, the plateau region may be affected by silicon and phosphorus due to that the region temperature corresponds to the maximum temperature (T3m) of the P–PU polymers and the maximum temperature (T2m) of the Si–PU polymers.

The TG curve of PDM22 with a PTMG chain length of 2000 also exhibits three weight-loss regions [Fig. 10(a)] that reflect a smaller split mul-

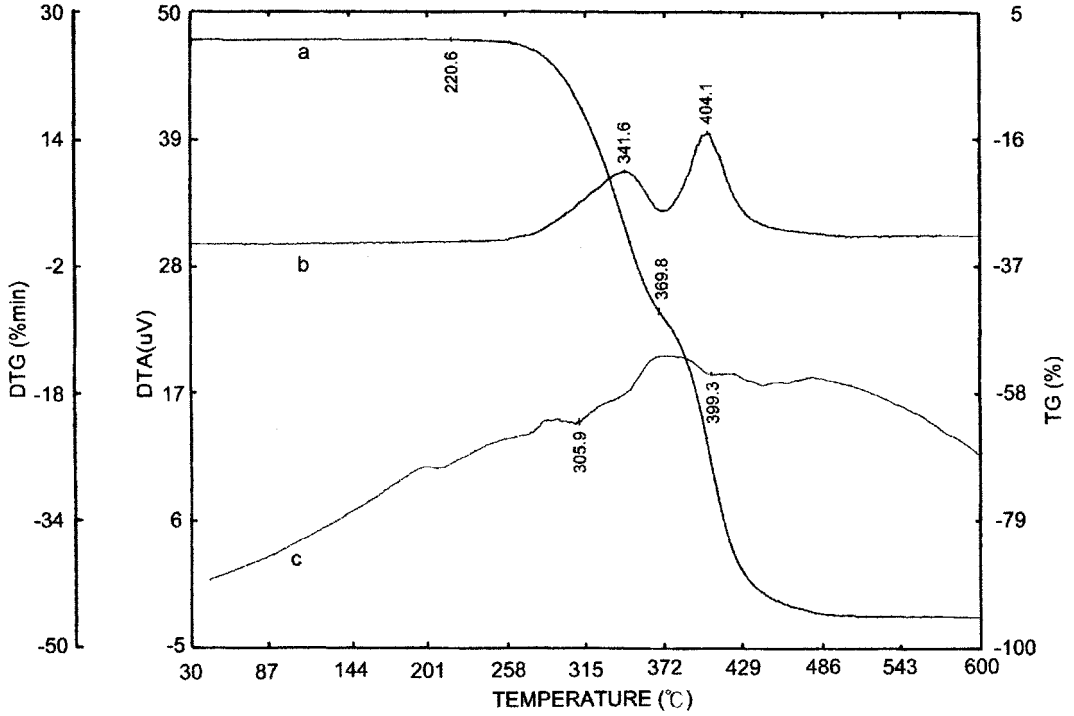

Figure 2 (a) TGA, (b) DTG, and (c) DTA curves of sample PU1 at a heating rate of 10°C under a nitrogen atmosphere.

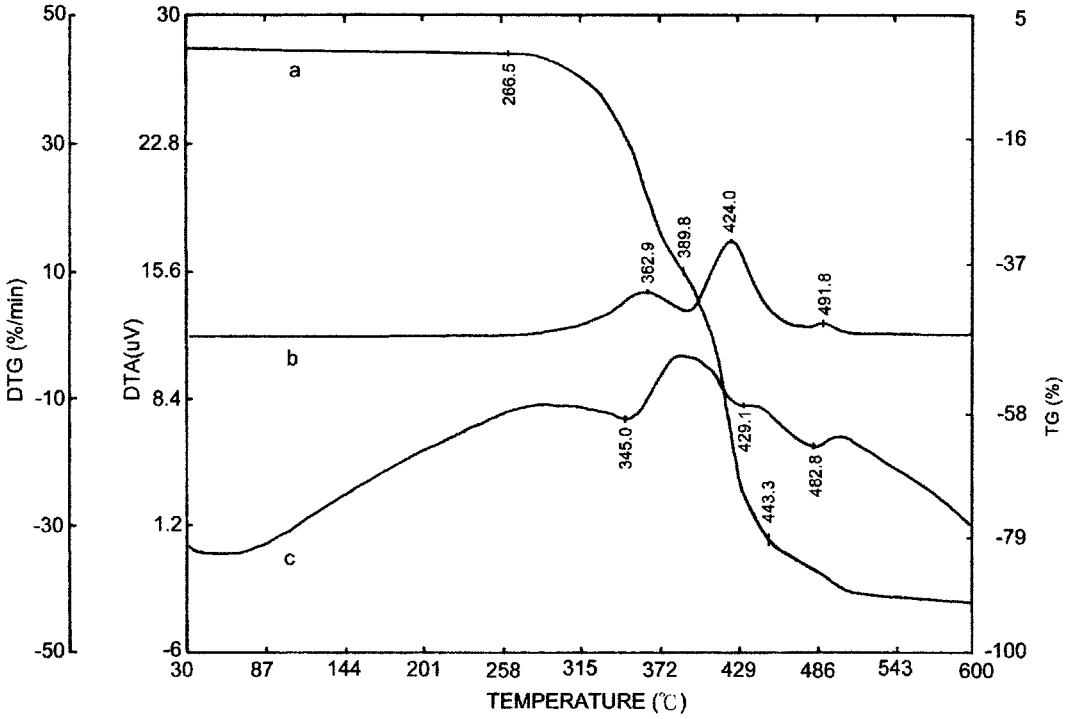

Figure 3 (a) TGA, (b) DTG, and (c) DTA curves of sample PD11 at a heating rate of 10°C under a nitrogen atmosphere.

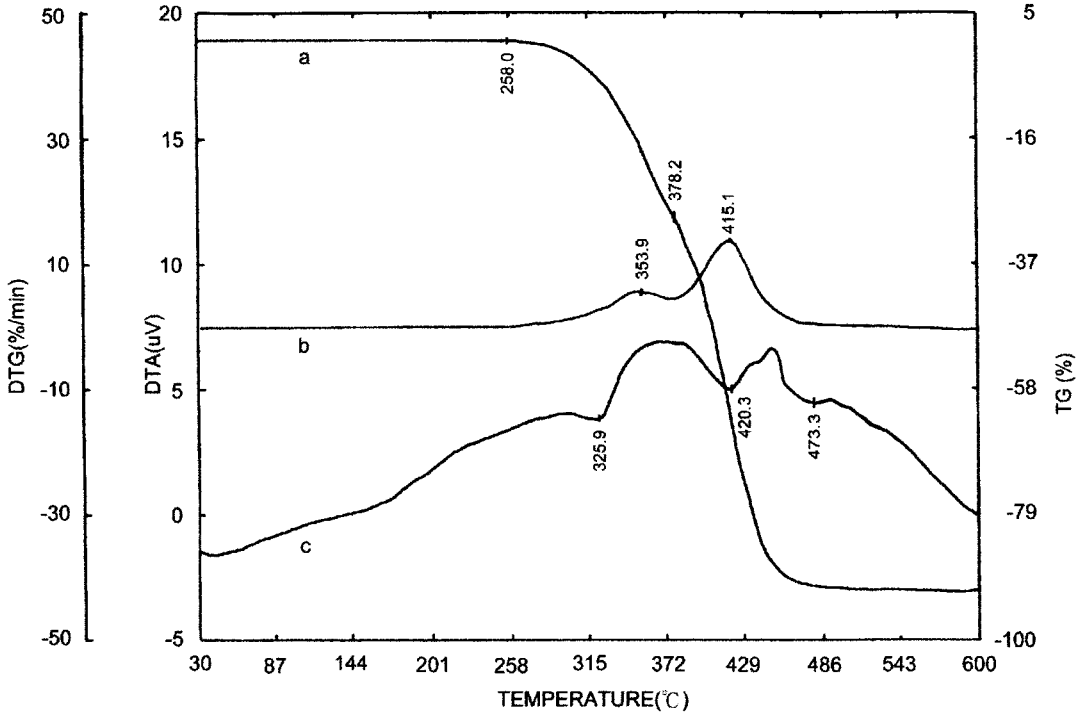

Figure 4 (a) TGA, (b) DTG, and (c) DTA curves of sample PD21 at a heating rate of 10°C under a nitrogen atmosphere.

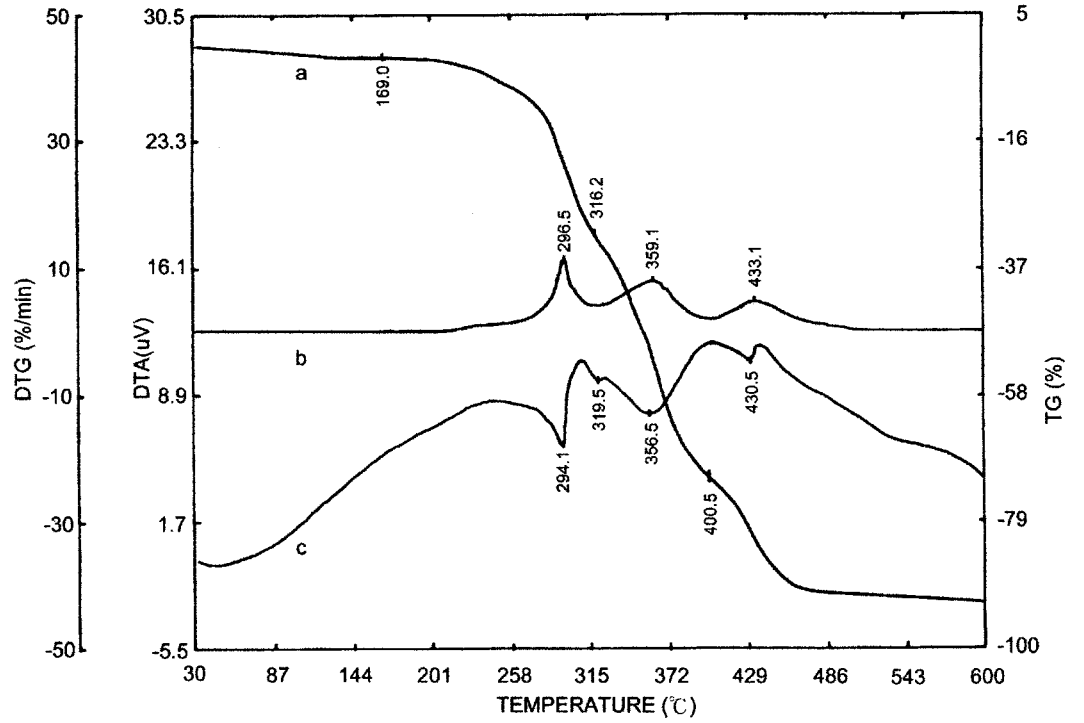

Figure 5 (a) TGA, (b) DTG, and (c) DTA curves of sample PM11 at a heating rate of 10°C under a nitrogen atmosphere.

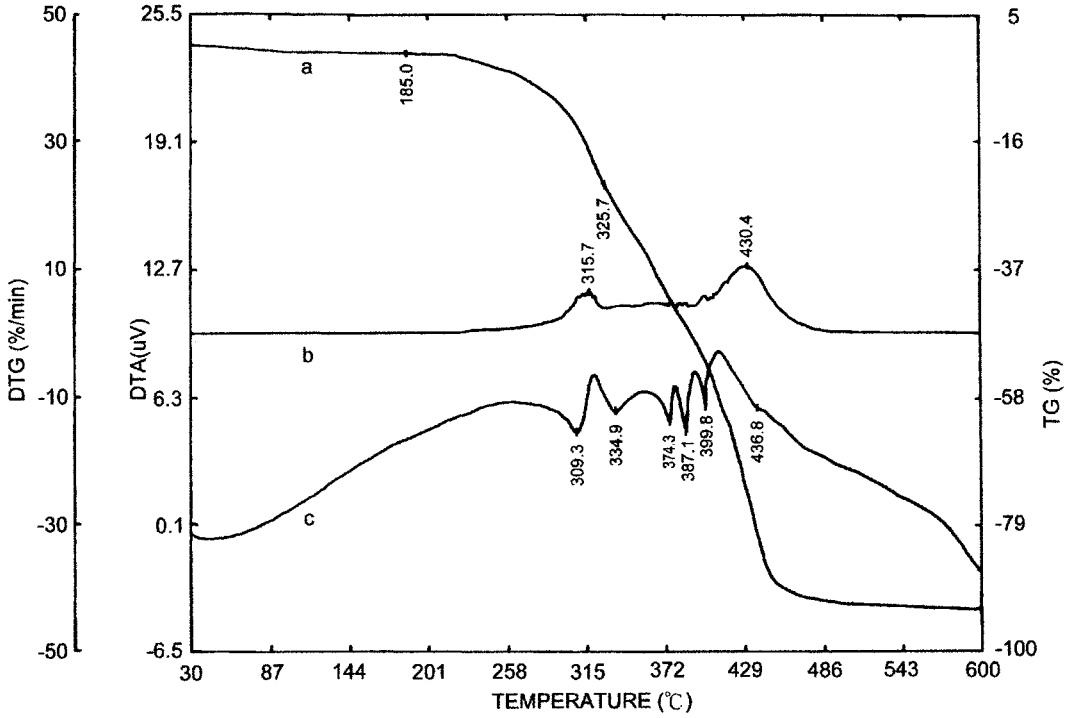

Figure 6 (a) TGA, (b) DTG, and (c) DTA curves of sample PM21 at a heating rate of 10°C under a nitrogen atmosphere.

tipeak and a smaller shoulder than that of the PDM12 as presented in Figure 10(b). Moreover, the DTA curve [Fig. 10(c)] displayed a three-region multiabsorption peak that differs from the PDM12 due to the phosphorus content and the chain length of the soft segments. An absorption peak was detected in the DTA curve for PDM12 and PDM22 above 429°C as displayed in Figures 9(c) and 10(c), which represented the decomposition of the silicon-containing segment.

Table III(d) confirms that the qualitative characterization of the Si–P–PU polymers is between that of pure PU and the Si–PU polymers. Furthermore, those Si–P–PU polymers with a higher silicon content have a higher T1on, T2on, and T1m. The T1on of Si–P–PU adopting PTMG 2000 (Si–P–PU2) was higher than that of the Si–P–PU polymers adopting PTMG 1000 (Si–P–PU1), whereas the T2on and T1m were reversed.

A simple maximum temperature of the second step (T2m) for those Si–P–PU polymers is difficult to determine on the DTG curves since the DTG curves exhibit a multipeak, a plateau range, and a shoulder. Therefore, a new symbol (Tm2–3) was employed in the degradation stage. The Tm2–3 may indicate the temperature of the maximum degradation rate for the Si–P–PU polymers between the second and the third steps, which is affected by the silicon and phosphorus content. Table III(d) confirms that the Tm2–3 is higher than the Tm2 of the P–PU1 polymers and is lower than the T2m of the Si–PU polymers. The DTG curves of the Si–P–PU polymers combined the effects of silicon and phosphorus according to the above discussion. Moreover, the TG curves seemingly display three weight-loss regions and the DTA curves can still exhibit the character of degraded absorption peaks of the Si–PU and P–PU polymers when the PU incorporates the silicon and phosphorus.

Kinetic Analysis

The kinetics of the degradation process was characterized by measuring the activation energy (Ea), which could be calculated by the isoconversional method. This method proposed by Ozawa[37] requires several TG curves at different heating rates. Figure 11 plots the relationship of the logarithm of the heating rate ($\log_{10} B$) versus $1/T$ for each value of α (α, degree of conversion = weight loss at a given temperature/total weight loss of the degradation) for the PD11 polymer. Usually, α was taken to be 0.1, 0.2, . . . 0.9. The activation

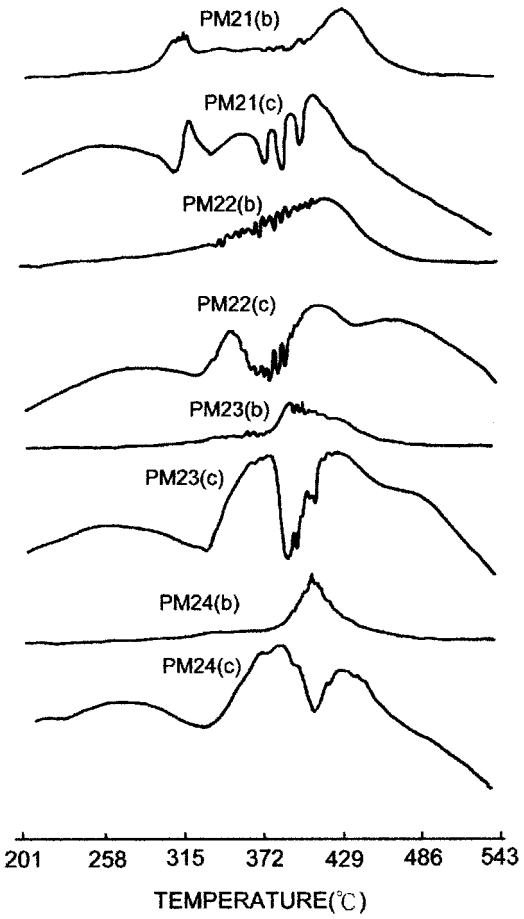

Figure 7 (b) DTG and (c) DTA curves of various phosphorous contents P-PU2 polymers at a heating rate of 10°C under a nitrogen atmosphere.

energy (Ea) was calculated for each conversion from these isoconversion curves and the value (Ea,av) of each degradation stage was averaged over the whole range of conversion (90%). Since these straight lines display excellent linearity for the Si–PU and P–PU polymers such as PD11 (Fig. 11), the Ea of those polymers was calculated from the slope of the lines applying the expression[37]

$$Ea = -\text{slope} \times R/0.457 \quad (1)$$

where R is the gas constant.

The Ea and Ea,av of various degradation stages of the samples are displayed in Table IV(a–c). The Ea exhibited a higher value at a high conversion and there was a near Ea value at the same degradation stage. The Ea had a large change in various degradation stages. Thus, the mechanism (chemical-bond breakage) of the degradation stage differs from that of other stages. However, the Ea value at the same degradation stage is somewhat distinct, confirming that the thermal degradation is a complex process. Grassie[22,38] discussed the degradation of PU and PU containing phosphorus by the Sub-Ambient Thermal Volatilization Analysis (SATVA) system. The thermal degradation mechanism was also very complex in that study and the chemical mechanism had more than three steps. The thermal degradation steps were previously deter-

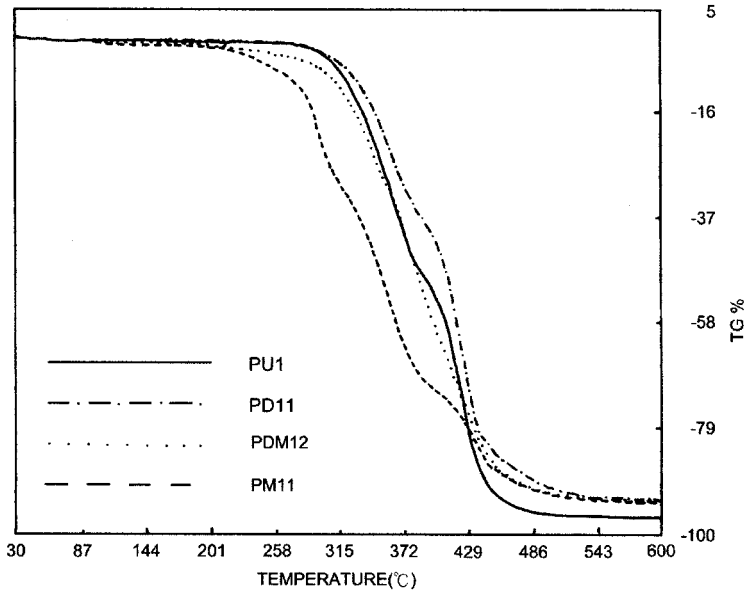

Figure 8 TGA curves of samples PU1, PD11, PDM12, and PM11 at a heating rate of 10°C under a nitrogen atmosphere.

Table III Characteristic Temperature of Pure PU, Si–PU, P–PU, and Si–P–PU on TGA Curves at 10°C/min Heating Rate Under Nitrogen Atmosphere

Code	T1on (°C)	T1m (°C)	T2on (°C)	T2m (°C)	T3on (°C)	T3m (°C)	Yc[b] (wt %)
				(a) Pure PU[a]			
PU1	220.6	341.6	369.8	404.1	—	—	3.9
PU2	221.7	330.6	364.5	400.3	—	—	2.8
				(b) Si–PU[a]			
PD11	266.5	362.9	389.8	424.0	443.2	491.8	9.8
PD12	253	350.0	386.3	424.1	435.2	487.1	8.7
PD13	250.9	350.7	386.2	421.6	430.3	486	7.8
PD14	240.9	354.9	387.1	424.1	438.7	483	7.1
PD21	258.0	353.9	378.2	415.1	—	—	7.9
PD22	245.5	352.7	373.7	413	—	—	7.2
PD23	234.1	355.2	377.0	412	—	—	6.9
PD24	230.5	350.6	377.3	413.9	—	—	6.3
				(c) P–PU[a]			
PM11	169.0	296.5	316.2	359.1	400.5	433.1	9.1
PM12	177.8	315.7	328.5	360.8	405.8	433.0	8.3
PM13	179.8	354.0	356.1	368.0	407.6	431.8	7.5
PM14	190.3	357.7	375.6	388.4	409.4	425.3	7.0
PM21	185.0	315.7	—	—	425.1	430	7.5
PM22	192.1	—	—	—	—	411.3	7.1
PM23	192.4	—	—	—	—	401.3	6.3
PM24	204.5	—	—	—	—	407.5	5.5
				(d) Si–P–PU[a]			
PDM11	206.2	350.1	365.0	407.5	9.7		
PDM12	201.1	348.9	357.8	382.0	10.1		
PDM13	193.3	338.6	350.1	429.2	10.3		
PDM21	245.1	340.1	363.8	405.0	8.5		
PDM22	213.5	339.9	356.0	402.4	9.2		
PDM23	192.7	328.1	334.8	388.4	9.4		

[a] The characteristic temperature is the onset and maximum temperature of the first step, T1on and T1m, and the same for the second step, T2on and T2m, and the third step, T3on and T3m.
[b] Yc = char residue at 500°C.
[c] Tm2–3: the maximum temperature in the second step of Si–P–PU polymer.

mined by TGA, which did not correspond to the thermal degradation mechanism determined by SATVA.

PU Polymers

The Ea of PU at various conversions (α) is presented in Table IV(a). There are two clear ranges in the Ea values of PU1: The Ea of the first region (stage I: $0.1 \leq \alpha \leq 0.4$) was between 138 and 120 kJ/mol, while the Ea of the second region (stage II: $0.5 \leq \alpha \leq 0.9$) was between 144 and 158 kJ/mol. Therefore, PU1 has at least two stages of degradation that correspond to the TGA result. The average Ea value of stage I (Ea,av1) and stage II (Ea,av2) expresses the degradation energy at various degradation stages as presented in Table V(a). Moreover, PU2 produced the same results as those of PU1, while the Ea of PU2 had a higher Ea in stages I and II.

Si–PU Polymers

Table IV(b) confirms that the Ea of the Si–PU polymers increased with increase of α and the DSiD content. Moreover, the Ea of the Si–PU polymers at $\alpha = 1$ was slightly higher than that of the pure PU at the same molecular weight of PTMG. However, the Ea of the Si–PU polymers was obviously higher than that of the pure PU at ≥ 0.1. According to our results, the silicon-containing urethane segment increases the Ea of the thermal degradation processes, especially when the thermal degradation occurs at a high conversion. Comparing the effect of different soft segments for the Si–PU polymers reveals that the Ea

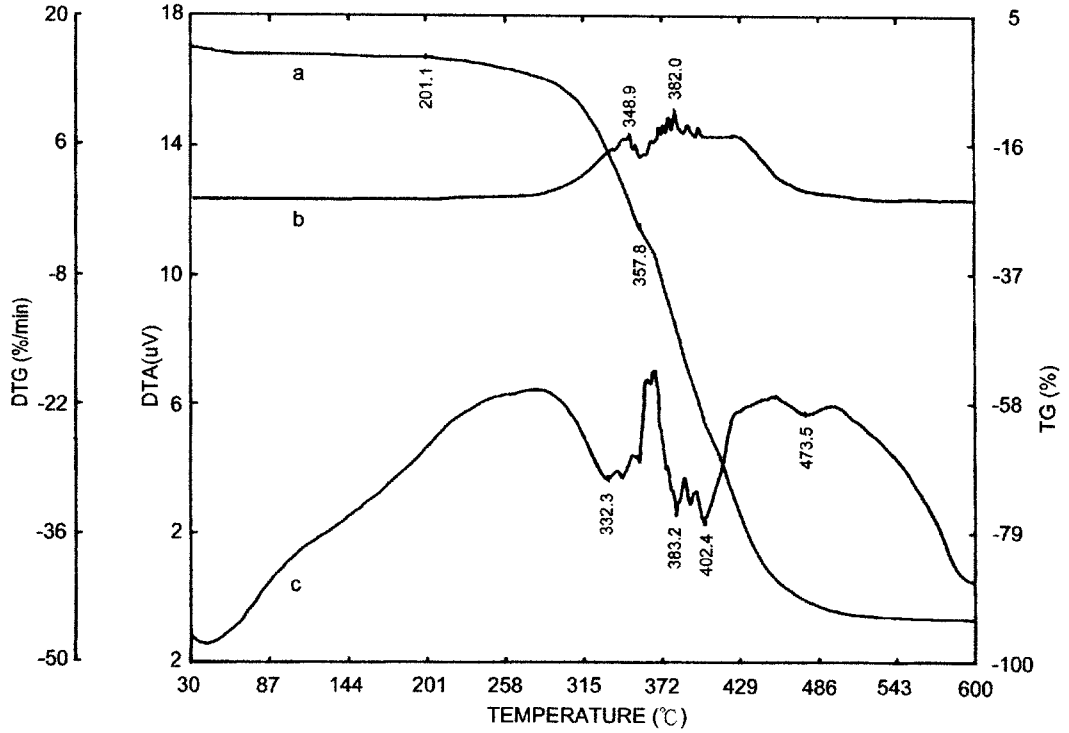

Figure 9 (a) TGA, (b) DTG, and (c) DTA curves of sample PDM12 at a heating rate of 10°C under a nitrogen atmosphere.

of the Si–PU1 polymers exceeded that of the Si–PU2 polymers. Furthermore, the Ea value of the Si–PU1 polymers in the range of $0.1 \leq \alpha \leq 0.9$ displayed three regions, while those of pure PU exhibited two regions.

The Ea of stage I ($0.1 \leq \alpha \leq 0.3$) and stage II ($0.4 \leq \alpha \leq 0.7$) for the Si–PU1 polymers with various silicon contents were higher than those of the pure PU. The Ea of the third region (stage III) was exhibited in the region of $0.8 \leq \alpha \leq 0.9$ for the Si–PU polymers, which corresponded to the third stage of the TGA measurement. Table V(b) reveals that the Ea,av1 and Ea,av2 of the Si–PU1 polymers were far higher than those of the pure PU. Moreover, PD11, with the maximum silicone content, has the highest Eav, av1 and Eav, av2. However, the Ea's of PD12, PD13, and PD14 are close at the same degradation stage. The Ea average of the third region (Ea,av3) of the Si–PU1 polymers was slightly higher than were the Ea,av1 and Ea,av2 around 194–237 kJ/mol. Similarly, the PD11 had the highest Ea,av3. The Ea value of the Si–PU2 polymers displayed only two regions (stage I: $0.1 \leq \alpha \leq 0.5$ and stage II: $0.6 \leq \alpha \leq 0.9$), which also corresponded to the TGA measurement. Table V(a,b) demonstrates that the Ea,av of the Si–PU1 polymers are higher than are those of PU at stages I and II. Moreover, the Ea and Ea,av of the Si–PU1 polymers were lower than were those of the Si–PU2 polymers for each stage. This result is opposite to that of the pure PU because the Si–PU1 polymers have more silicone-containing urethane segments than have the Si–PU2 polymers. The Si–PU polymers are more thermally stable, particularly when the degradation approaches high conversion, since the Si–PU polymers also have a higher Ea than that of PU at any conversion or each stage of degradation. The high thermal stability clearly resulted from the silicon compound that formed during the degradation processes.[39]

P–PU Polymers

Table IV(c) indicates that the Ea of the P–PU polymers with various phosphorus contents around 98–120 kJ/mol at $\alpha = 1$ was significantly lower than that of the pure PUs' Ea and the Si–PU polymers' Ea. Moreover, the Ea of the P–PU polymers increased as the conversion increased. The thermal stability of the P–PU polymers was the lowest at $\alpha = 1$ compared with pure

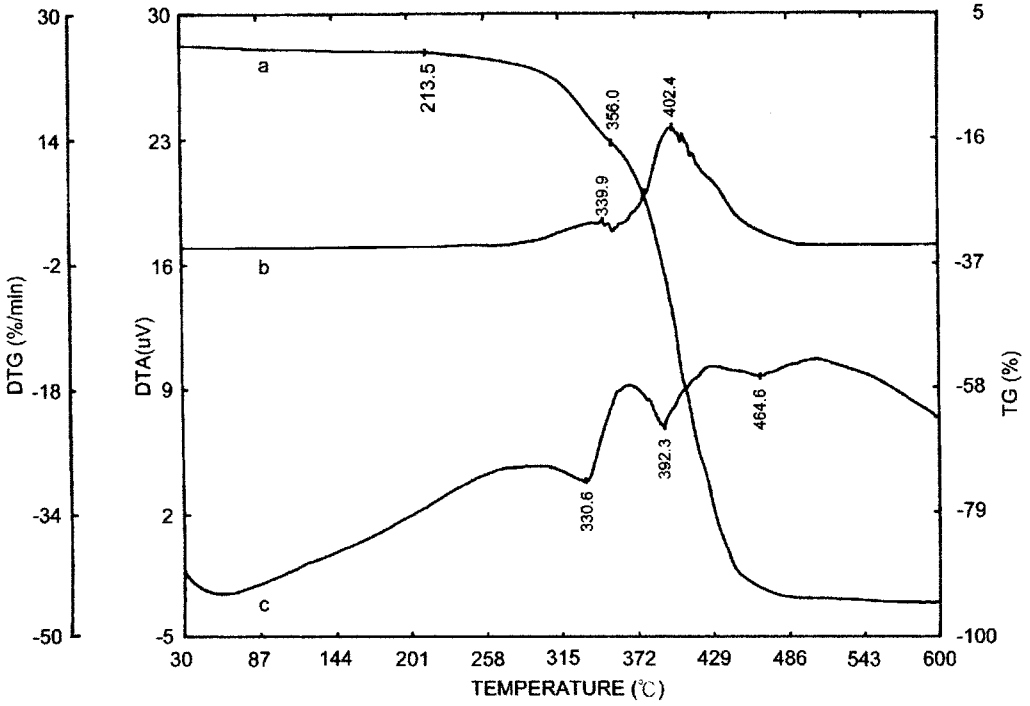

Figure 10 (a) TGA, (b) DTG, and (c) DTA curves of sample PDM22 at a heating rate of 10°C under a nitrogen atmosphere.

PU and the Si–PU polymers. The low *Ea* was probably due to the presence of the P—O—C structure in the main chain, which is susceptible to chain scission during thermal degradation and acts as a weak link.[40] Otherwise, the *Ea* of the P–PU polymers increased in the range of $0.4 \leq \alpha \leq 0.5$ and decreased as the phosphorus content increased in the range of $0.1 \leq \alpha \leq 0.5$. However,

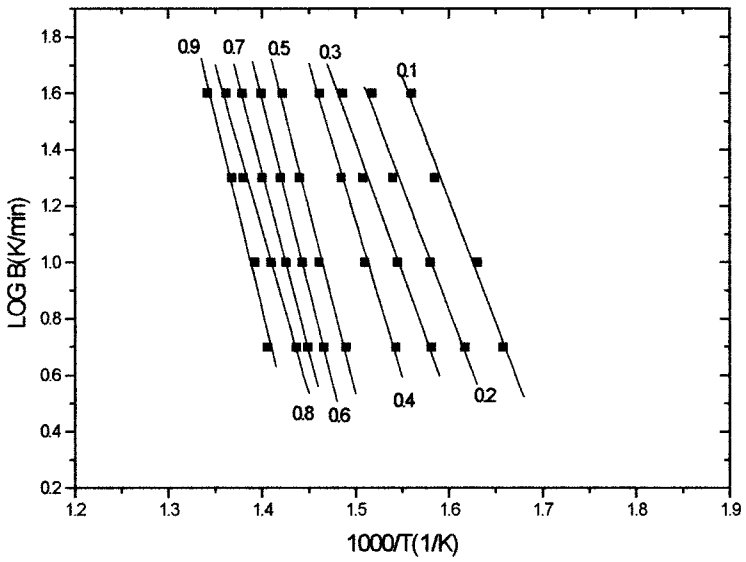

Figure 11 Dependence of the logarithm of the heating rate (Log B) versus the reciprocal absolute temperature ($1/T$) for the Ozawa method at the indicated conversion (α) of decomposition of PD11 in nitrogen.

Table IV Activation Energies (*Ea*) in kJ/mol of the PU, Si–PU, P–PU, and Si–P–PU Degradation Processes Calculated by the Ozawa Method

	Conversion (α)								
	0.1	0.2	0.3	0.4	0.5	0.6	0.7	0.8	0.9
Code	Stage I[a]						Stage II[a]		
				(a) PU					
PU1	150	137	120	127	144	151	147	158	150
PU2	134	132	137	148	162	171	156	169	168
				(b) Si–PU					
		Stage I[a]			Stage II[a]			Stage III[a]	
PD11	159	160	168	202	240	249	212	231	243
PD12	155	159	160	182	190	202	204	206	202
PD13	154	163	160	181	186	205	202	209	205
PD14	151	156	145	182	189	203	199	193	194
			Stage I[a]				Stage II[a]		
PD21	152	161	170	170	169	176	188	184	191
PD22	151	160	169	163	163	174	178	175	176
PD23	146	155	161	156	152	168	170	173	172
PD24	140	150	151	157	165	166	170	170	167
				(c) P–PU					
		Stage I[a]			Stage II[a]			Stage III[a]	
PM11	98	101	111	111	167	196	202	215	249
PM12	108	105	117	118	165	194	204	208	218
PM13	111	108	118	120	161	195	203	209	207
PM14	118	109	121	121	158	177	196	201	183
		Stage I[b]				Stage II[b]		Stage III[b]	
PM21	115	116	127	147	168	190	192	194	204
PM22	116	119	120	148	179	195	208	198	193
PM23	118	126	129	146	173	175	198	199	192
PM24	120	122	134	150	170	173	177	183	183
				(d) Si–P–PU					
PDM11	153	155	165	183	201	231	—	—	—
PDM12	148	155	173	203	—	—	—	—	—
PDM13	132	144	147	149	209	—	—	—	—
PDM21	133	146	176	181	198	231	224	232	231
PDM22	150	147	164	169	188	189	215	219	—
PDM23	141	144	152	154	—	—	—	—	—

[a] The first, second, and third stage of degradation, Stage I, Stage II, and Stage III, determined by TGA and kinetics.
[b] The first, second, and third stage of degradation, Stage I, Stage II, and Stage III, determined only by kinetics.

there was a reverse tendency in the range of $0.6 \leq \alpha \leq 0.9$. The *Ea* of a rapid increase and a reverse tendency may be attributed to the formation of a thin glassy layer. Comparing the *Ea* of the P–PU polymers employing various molecular lengths of the soft segment reveals that the P–PU polymers with a long soft segment have higher *Ea* values in various stages of thermal degradation. The *Ea* value of the P–PU1 polymers in the range of $0.1 \leq \alpha \leq 0.9$ also exhibits three distinct regions, which also correlate with the TGA result. Table V(c) demonstrates that the *Ea*,av1 of stage I ($0.1 \leq \alpha \leq 0.4$) was substantially lower than that of PU1 and Si–PU1, which verifies that the P–PU1 polymers have a lower thermal stability at stage I. However, the *Ea*,av2 of the P–PU1 polymers was higher than that of PU1 and slightly lower than that of the Si–PU1 polymer at stage II ($0.5 \leq \alpha \leq 0.7$). Moreover, the *Ea*,av3 of stage III ($0.8 \leq \alpha \leq 0.9$) was roughly the same as that of the Si–PU1 polymers. Stages II and III possessed a higher *Ea* because a thermal stable thin glassy layer of polyphosphate was formed in these stages, which corre-

Table V PU, Si–P, and P–PU of Average of *Ea* of Various Degradation Stages

Code	Average of *Ea* for Various Degradation Stages (kJ/mol)		
	Stage I (*Ea*,av1[a])	Stage II (*Ea*,av2[b])	Stage III (*Ea*,av3[c])
	(a) PU		
PU1	134	150	—
PU2	138	165	—
	(b) Si–PU		
PD11	172	234	237
PD12	164	197	204
PD13	164	198	207
PD14	159	197	194
PD21	164	184	—
PD22	161	176	—
PD23	154	171	—
PD24	153	168	—
	(c) P–PU		
PM11	103	169	232
PM12	110	170	213
PM13	112	170	208
PM14	116	163	192

[a] *Ea*,av1: Average *Ea* of the first stage.
[b] *Ea*,av2: Average *Ea* of the second stage.
[c] *Ea*,av3: Average *Ea* of the third stage.

sponded to the TGA system. Although the *Ea* values of the P–PU2 polymers based on the kinetic analysis can be divided into three ranges, the second and third stages of the P–PU2 polymers are difficult to determine on the TG and DTG curves. Therefore, the average *Ea* for each degraded stage was not calculated.

Si–P–PU Polymers

The *Ea* values of the Si–P–PU polymers are not meaningful above a 50% weight loss since the *Ea* values undergo great changes at high conversion. Therefore, only some *Ea*'s could be calculated [Table III(d)] since most samples had a poor relationship between the graph of log B and $1/T$. Thus, to reach a definite conclusion on the effects of the silicon and phosphorus content at high conversion is extremely difficult. The average *Ea* for various stages of degradation was also undetermined for the Si–P–PU polymers. However, the samples employing the same PTMG molecular weight have a higher *Ea* than that of P–PU and the activation energies were roughly the same as was the *Ea* of the Si–PU polymers at low conversion ($0.1 \leq \alpha \leq 0.4$). Thus, the *Ea* of the Si–P–PU polymers has a suitable thermal stability due to the temperature of the onset degradation and proximity of the *Ea* to the pure PU.

CONCLUSIONS

This work presented a two-step process capable of synthesizing a series of Si–PU polymers, P–PU polymers, and Si–P–PU. The ^{1}H-NMR demonstrated the structures and character of those polymer groups. Moreover, the ^{1}H-NMR spectrum measured the ratio of the integral amplitudes between the urethane linkage protons and the methylene protons of MDI, which can quantitatively analyze those polymers. The TG–DTG–DTA curves determined the thermal stability of those polymers during the degradation processes. The Si–PU series polymers have higher thermal stability at each degradation step since the silicon-containing segment is more thermally stable. On the contrary, the P–PU series polymers are less stable since the phosphorus-containing segment easily degrades. The effect of the synergism of silicon and phosphorus during degradation processes should be considered since the DTG curves of the Si–P–PU polymers combine the temperatures of the characteristic degradation of the Si–PU polymers and P–PU polymers. Moreover, the *Ea* and *Ea*,av measurements supported the results of the TG–DTG–DTA curves. The *Ea* or *Ea*,av at various degradation stages provides auxiliary data about the thermal stability of the examined polymers when the characteristic degradation temperatures are difficult to determine from the TG–DTG–DTA curves.

The authors would like to thank the National Science Council of the Republic of China for financially supporting this research under Contract No. 87-2216-E-238-003.

REFERENCES

1. Hepburn, C. Polyurethane Elastomers; Applied Science: London and New York, 1982; pp 1–2.
2. Woods, G. The ICI Polyurethanes Book; I.C.I./ Wiley: New York, 1987; pp 1–6.
3. Oertel, G. Polyurethane Handbook; Hanser: Munich, Vienna, New York, 1985; pp 577–590.
4. Petrovic, Z. S.; Zavargo, Z.; Flynn, J. H.; Macknight, W. J. J Appl Polym Sci 1994, 51, 1087.

5. Masiulanis, B.; Zielinski, R. J Appl Polym Sci 1985, 30, 2731.
6. Lin, M. F.; Chuang, F. S.; Shu, Y. C.; Tsen, W. C. Polym Int 1999, 48, 433.
7. Mikroyannidis, J. A. J Polym Sci Part A Polym Chem 1998, 26, 885.
8. Beachel, H. C.; Ngoc Son, C. P. J Appl Polym Sci 1963, 7, 2217.
9. Dye, E.; Hammond, R. J. J Appl Polym Sci 1972, 8, 1499.
10. Ferguson, J.; Petrovic, Z. Eur Polym J 1976, 12, 177.
11. Lin, M. F.; Wang, H. H.; Chuang, F. S.; Shu, Y. C.; Tsen, W. C. J Polym Res 1996, 3, 105.
12. Kotomkin, V. Y.; Baburina, A. V.; Lebedov, E. P.; Bylev, V. A.; Yasmikova, T. E.; Reikhsfeld, V. O. Khim Parki Primonenie Krem Fosforogan Soedin L 1980, 23; Chem Abstr 1980, 95, 43841d.
13. Kotomkin, V. Y.; Baburna, V. A.; Lebdev, V. P.; Kercha, Y. Y. Plast Massy 1981, 27; Chem Abstr 1981, 95, 43841d.
14. Kuznetsova, V. P.; Zapunnaya, K. USSR Patent 422246 (1978); Chem Abstr 1998, 90, 7759W.
15. Lewin, M.; Atlas, S. M.; Pearce, E. M. Flame-Retardant Polymeric Materials; Plenum: New York, 1975; pp 1–15.
16. Turi, A. E. Thermal Characterization of Polymeric Materials; Academic: London, 1981; pp 794–796.
17. Kambour, R. P.; Klopfer, H. J.; Smith, S. A. J Appl Polym Sci 1981, 26, 847.
18. Benrashid, R.; Neison, G. L. J Polym Sci Part A Polym Chem 1994, 32, 1847.
19. Chang, T. C.; Chen, Y. C.; Ho, S. Y.; Chiu, Y. S. Polymer 1996, 37, 2963.
20. Sava, I.; Bruma, M.; Schulz, B.; Mercer, F.; Reddy, V. N.; Belomoina, N. J Appl Polym Sci 1997, 65, 1533.
21. Chang, T. C.; Wu, J. H. Polym Degrad Stab 1998, 60, 161.
22. Grassie, N. Polym Eng Sci 1982, 22, 1057.
23. Reghunadhan Nair, C. P.; Clouet, G.; Guilbert, Y. Polym Degrad Stab 1989, 26, 305.
24. Liu, Y. L.; Hsiue, G. H.; Lee, R. H.; Chiu, T. S. J Appl Polym Sci 1997, 63, 895.
25. Ma, Z.; Zhao, W.; Liu, Y.; Shi, J. J Polym Appl Sci 1997, 63, 1511.
26. Cheng, T. C.; Chiu, Y. S.; Chen, H. B.; Ho, S. Y. Polym Degrad Stab 1995, 47, 375.
27. Fridman, I. D.; Thomas, E. L. Polymer 1980, 21, 393.
28. Hepburn, C. Polyurethane Elastomers; Applied Science: London and New York, 1982; p 316.
29. Saunders, J. H. Rubb Chem Technol 1959, 32, 337.
30. Ballistreri, A.; Foti, S.; Maravigna, P.; Montaudo, G.; Scamperrino, E. J Polym Chem Ed 1980, 18, 1923.
31. Grassie, N.; Macfarlans, I. G. Eur Polym J 1978, 14, 875.
32. Bannister, D. J.; Semlyen, J. A. Polymer 1981, 22, 377.
33. Thomas, T. H.; Kendrick, T. C. J Polym Sci Part A 2 1969, 7, 537.
34. Green, J. J Fire Sci 1992, 10, 470.
35. Troev, K.; Kisiova, T.; Grozeva, A.; Borisov, G. Eur Polym J 1993, 1211.
36. Hilado, C. J Cell Plast 1968, 4, 339.
37. Ozawa, T. Bull Chem Soc Jpn 1965, 38, 1881.
38. Norman, G. Polym Degrad Stab 1990, 30, 3.
39. Allen, S. N.; Edge, M. Fundamentals of Polymer Degradation and Stabilization; Elsevier: UK, 1992; p 8.
40. Montaudo, G.; Puglisi, C.; Scamporrino, E.; Vitalini, D. Macromolecules 1984, 17, 1605.